Monte Carlo Study of the Relative Frequency of Scattering Processes in Si-Inversion Layers

V.M.Borzdov[1], V.O.Galenchik[1], H.Kosina[2], F.F.Komarov[1], O.G.Zhevnyak[1]

[1] *Belarus State University, Fr.Skarina av. 4, 220050 Minsk, Belarus,*

[2] *Institute for Microelectronics, TU Vienna, Gusshausstrasse 27-29/E360 A-1040 Vienna, Austria*

(Received 8 April 2003, accepted for publication 28 April 2003)

Self-consistent Monte Carlo simulation of the two-dimensional (2D) electron transport in Si-inversion layers has been performed to study the relative frequency of scattering processes. Intra- and intersubband scattering by intervalley and acoustic phonons, impurity scattering, electron-electron scattering, and surface roughness scattering were taken into account. The simulation was made at the temperatures $T = (77 \div 350)$ K, the sheet electron densities $N_s = (10^{16} \div 10^{17})$ m^{-2}, and the driving electric field strengths $F = (10^5 \div 10^7)$ V/m. The ratios of the partial number of scattering events of each considered process to the whole number of scattering events were studied as quantitative measures.

1. Introduction

Because of the wide utilization of Si-MOSFETs as elements of ICs the investigation of the features of the electron transport in inversion layers of these structures is very important. It is well known that the thickness of the inversion layer is comparable with the charge carrier de Broglie wavelength so that the quantization of electron energy in the direction perpendicular to the surface takes place [1]. This circumstance strongly influences the electron transport in 2D structures. It is known that this transport is significantly determined by the dominant 2D electron scattering processes. In this connection a comparative analysis of the partial influence of each dominant scattering process on the electron kinetics in a wide range of temperatures, sheet electron densities, and driving electric field strength values is of great interest. This analysis can be carried out using the Monte Carlo transport simulation because this technique

allows one to take into account all dominant scattering mechanisms in the inversion layer under various conditions. The relative number of scattering events (RNSE) equal to the ratio of the number of scattering events of a particular process with respect to the total number of scattering events, can be used as a quantitative measure of the comparative influence of the scattering mechanisms on the 2D electron transport.

The purpose of this study is the self-consistent Monte Carlo simulation of 2D electron transport in Si-inversion layers taking into account the population of the six lowest subbands as well as the dominant scattering mechanisms and investigation of the partial contribution of the considered scattering processes at various temperatures, sheet electron densities, and tangential electric field strengths. The ensemble Monte Carlo simulation procedure [2] is used.

As in Refs. [3, 4, 5, 6], in the present study it is assumed that the inversion layer in a Si-MOS structure is in the (100) plane and the driving field is applied in the <110> direction.

2. The model

First of all the problem of a self-consistent calculation of energy levels and wave functions at various temperatures T and sheet charge carrier densities N_s is solved. The Schrödinger and Poisson equations and the boundary conditions are written as [1]

$$-\frac{\hbar^2}{2m_z}\frac{d^2\psi_n(z)}{dz^2} - e\phi(z)\psi_n(z) = E_n\psi_n(z), \tag{1}$$

$$\epsilon\epsilon_0\frac{d^2\phi(z)}{dz^2} = eN_s\sum_n N_n|\psi_n(z)|^2 - \rho_{depl}, \tag{2}$$

$$\psi_n(0) = \psi_n(z_{depl}) = 0, \tag{3}$$

$$\phi(0) = \phi'(z_{depl}) = 0. \tag{4}$$

Here m_z is the electron effective mass in the direction normal to the surface, $\hbar$ is the reduced Planck constant, $\psi_n(z)$ is the electron wave function in the n-th subband, E_n is the corresponding subband energy, $\phi(z)$ is the electrostatic potential, e is the electron charge, N_n is the relative occupation of the n-th subband, ρ_{depl} is the charge density in the depletion layer with the thickness z_{depl}, and $\epsilon_0\epsilon$ is the dielectric permittivity of silicon.

The solution of the equation set (1)–(4) is used to calculate the scattering rates in the Monte Carlo simulation procedure. We take into account intra- and

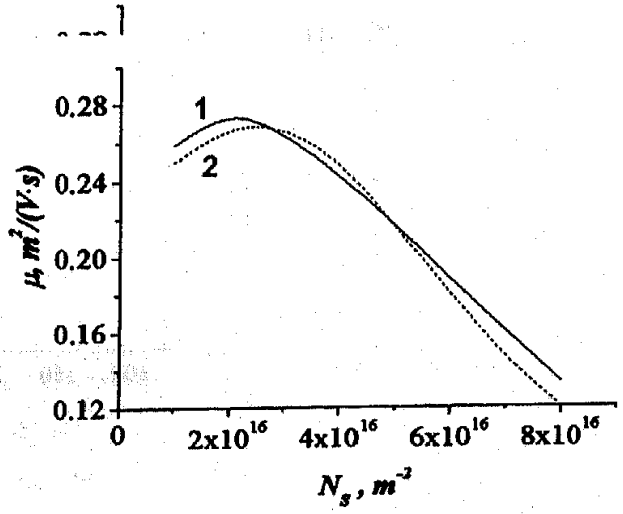

Figure 1. Electron mobility μ versus the sheet charge carrier density N_s at $N_{depl} = 1.5 \cdot 10^{15}\ m^{-2}$, $T = 77\ K$, $F = 10^4$ V/m. 1 – Monte Carlo simulation, 2 – experiment [10].

intersubband scattering by intervalley and acoustic phonons, impurity scattering, electron-electron scattering, and surface roughness scattering.

The rate of intra- and intersubband scattering by intervalley optical phonons from the subband with number m to the subband with number n is calculated according to [3, 4, 5, 6, 7, 8, 9, 10]

$$W_{mn}^{opt}(E) = \frac{g_n m_{dn}^* D_o^2}{\hbar^2 \rho \omega_{ph}} \frac{1}{2b_{mn}} (N + 1/2 \mp 1/2) u_0(E - E_n \pm \hbar\omega_{ph}), \tag{5}$$

where E is the electron energy, D_o is the coupling constant, g_n is the degeneracy of the final subband, $\hbar\omega_{ph}$ is the phonon energy, ρ is the mass density of silicon, N is the number of phonons with energy $\hbar\omega_{ph}$, E is the electron energy before the scattering, m_{dn}^* is the density-of-states effective mass in the n-th subband, u_0 is the unit step function,

$$\frac{1}{b_{mn}} = 2 \int |\psi_m(z)|^2 |\psi_n(z)|^2 dz. \tag{6}$$

The upper sign in Eq. (5) corresponds to phonon absorption and the lower one to phonon emission.

The rate of acoustic scattering is calculated according to [3, 4, 5, 6, 7, 8, 9, 10]

$$W_{mn}^{ac}(E) = \frac{m_{dn}^* D_a^2 k_B T}{\hbar^3 \rho s_l^2} \frac{1}{2b_{mn}} u_0(E - E_n), \tag{7}$$

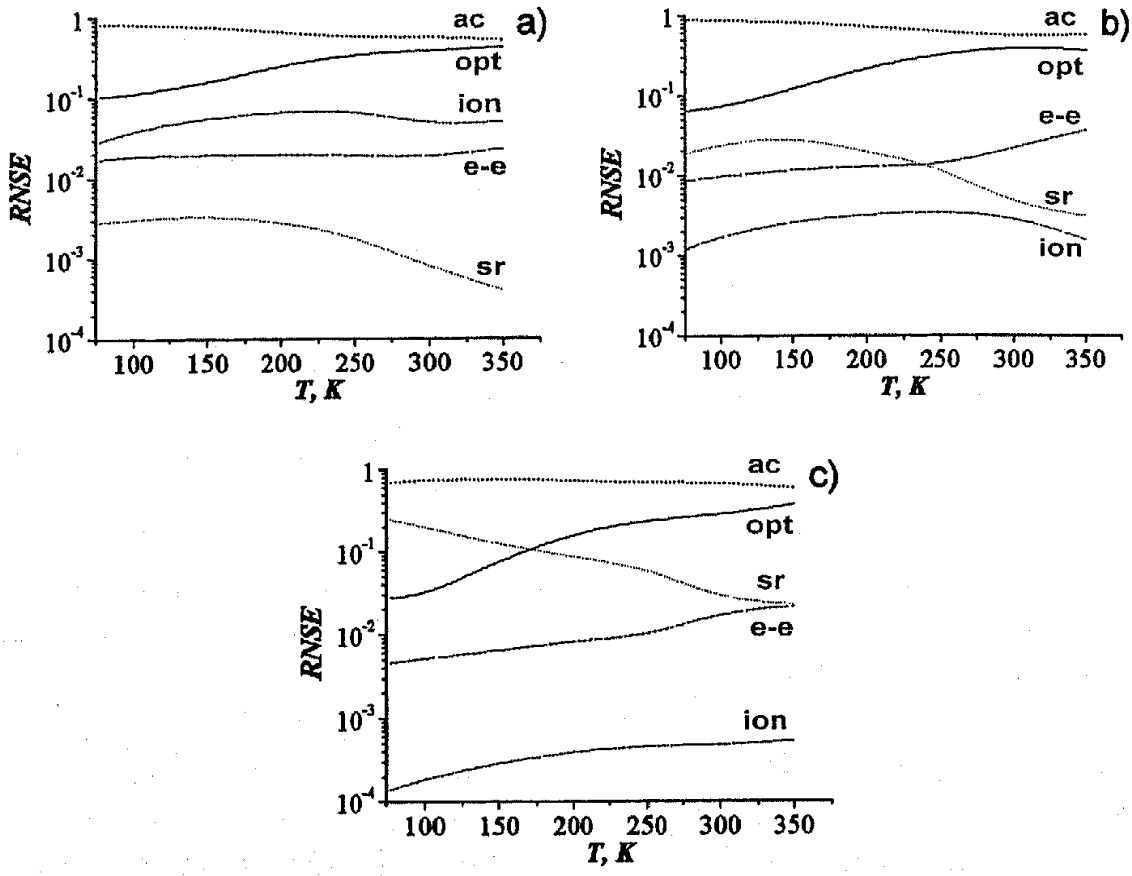

Figure 2. RNSE versus temperature T at $F = 10^5$ V/m and (a) – $N_s = 10^{16}$ m^{-2}, (b) – $N_s = 4 \cdot 10^{16}$ m^{-2}, (c) – $N_s = 10^{17}$ m^{-2}.

where D_a is the deformation potential of acoustic phonons, k_B is the Boltzmann constant, s_l is the sound velocity. Since the energy of acoustic phonons is small, acoustic scattering can be considered as an elastic scattering mechanism [3, 4, 5, 6, 7].

For the calculation of the ionized impurity scattering rate with the account of screening the Ning and Sah formula is used [11]

$$W^{ion}(E) = \frac{1}{2\pi\tau_0(E_{kin})} \int_0^{2\pi} (1 + s/q) d\theta, \tag{8}$$

where

$$\frac{1}{\tau_0(E_{kin})} = \frac{\pi^2 e^4 N_I}{256\tilde{\epsilon}^2\epsilon_0^2\hbar E_{kin}}, \tag{9}$$

E_{kin} denotes the electron kinetic energy, N_I the sheet concentration of ionized impurity, $q = 2k\sin(\theta/2)$, k the absolute value of the wave vector, $\tilde{\epsilon} = (\epsilon + \epsilon_{ox})/2$, ϵ_{ox} is the dielectric permittivity of SiO_2, and s is the screening factor which is

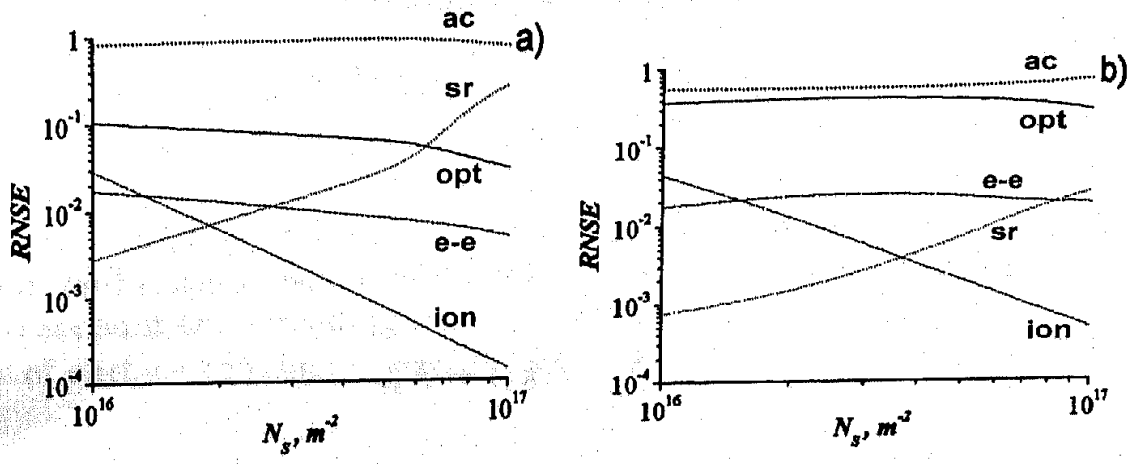

Figure 3. RNSE versus sheet charge carrier density N_s at $F = 10^5$ V/m and (a) – $T = 77$ K, (b) – $T = 300$ K.

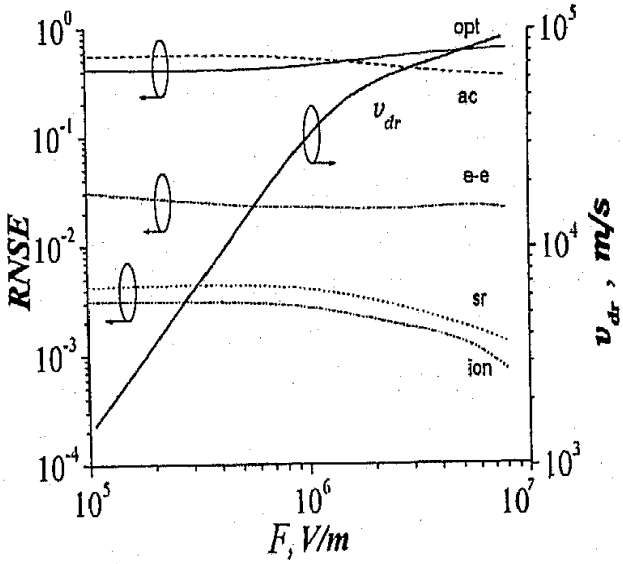

Figure 4. RNSE and drift velocity v_{dr} versus longitudinal electric field F at $N_s = 4 \cdot 10^{16}$ m^{-2} and $T = 300$ K.

equal to

$$s = \frac{2\pi e^2 N_s}{\epsilon\epsilon_0 k_B T}. \tag{10}$$

This scattering process is elastic. The scattering angle is selected according to the Neumann procedure with the distribution $f(\theta) \sim 2\pi(1 + s/q)$.

It is well known that the electron-electron (e-e) scattering in a 2D electron gas can cause intersubband transitions [12, 13]. According to Ref. [13] the total

e-e scattering rate from the subband i to subband j is equal to

$$W_{ij}^{e-e} = \frac{e^4 m_{dj}}{4\pi\hbar^3\epsilon^2\epsilon_0^2 A} \sum_{n,m,\vec{k_2}} f(\vec{k_2}) \int \frac{|F_{ijmn}(q)|^2}{(s+q)^2} dq, \tag{11}$$

where $\vec{k_2}$ is the wave vector of the second electron taking part in the scattering event, A is the scaling constant for the wave vector distribution function $f(\vec{k_2})$

$$\frac{1}{A} \sum_{n,m,\vec{k_2}} f(\vec{k_2}) = N_s, \tag{12}$$

$F_{ijmn}(q)$ is the form-factor

$$F_{ijmn}(q) = \int dz \int dz' \psi_i(z)\psi_m(z')\psi_j(z)\psi_n(z') \exp(-q|z-z'|), \tag{13}$$

m and n are the numbers of second electron subband before and after scattering, respectively, and $q = |\vec{k} - \vec{k'}|$, $\vec{k'}$ is the electron wave vector after scattering.

Direct calculation of the e-e scattering rate using Eq. (11) is complicated because the distribution function $f(\vec{k_2})$ has to be known. This function is *a priori* undefined and may by evaluated only from the self-consistent simulation procedure, which, however, is very CPU time consuming.

For the simulation of the e-e scattering we used the approach proposed in Ref. [13] and enhanced in Ref. [14] and applied also in Refs. [15, 16]. The integrand in Eq. (11) is maximized, i.e. $f(\vec{k_2})$ is replaced by its maximum value $1/s^2$. The actual value of the form-factor $F_{ijmn}(q)$ is taken into account in the final state selection. This approach is similar to the free flight time selection using the self scattering idea [2]. The rate of intrasubband e-e scattering is derived from Eq. (11)

$$W_{ii}^{e-e,max} = \frac{e^4 m_{di} N_s}{4\pi\hbar^3\epsilon^2\epsilon_0^2}. \tag{14}$$

Then the rate of intersubband e-e scattering is

$$W_{ij}^{e-e,max} = W_{ii}^{e-e,max} F_{max}^2 N_{sub}, \tag{15}$$

where $F_{max} = \max_{m,n,q} F_{ijmn}(q)$, N_{sub} is the number of subbands. In the simulation of an e-e scattering event it is assumed that the real scattering event takes place if the following condition is valid:

$$r\frac{1}{s^2} \leq \frac{|F_{ijmn}(q)|^2}{(s+q)^2}, \tag{16}$$

where r is a uniformly distributed random number in the range of [0,1]. If the condition (16) is not satisfied then self scattering takes place. The energy of the second electron is selected equal to the ensemble average energy at the current time. The direction of its wave vector is assumed to be random. Scattering for $|i-j|>1$ and $|m-n|>1$ is neglected because the values of the corresponding form-factors are very small [12, 14].

When the surface roughness scattering is considered it is very important to take into account the screening effect in 2D electron gas [1, 17, 18]. In this study the rate of surface roughness scattering is calculated according to [9, 16, 19]

$$W^{sr}(E)=\frac{m_d^* e^2 F_{eff}^2 \Delta^2 L^2}{2\hbar^3}\int_0^{2\pi}\frac{1}{\epsilon(q)}\exp\left(\frac{-q^2L^2}{4}\right)d\theta. \tag{17}$$

Here Δ is the rms. height and L is the correlation length of surface roughness, $F_{eff}=e(N_s/2+N_{depl})/\epsilon\epsilon_0$ is the effective field strength, and $\epsilon(q)$ is the dielectric function given by

$$\epsilon(q)=1+\frac{e^2}{2\epsilon\epsilon_0}\frac{1}{q}\frac{m_d^*}{\pi\hbar^2}I(q), \tag{18}$$

where

$$I(q)=\sum_i\int dz\int dz'|\psi_i(z)|^2|\psi_i(z')|^2\exp(-q|z-z'|). \tag{19}$$

The ranges of the values of L and Δ are selected according to the results of Ref. [20, 21]. Surface roughness scattering is an elastic process. The scattering angle is selected using the Neumann technique with the distribution function

$$f(\theta)\sim\frac{1}{\epsilon(q)}\exp\left(\frac{-q^2L^2}{4}\right). \tag{20}$$

The self-consistent Monte Carlo simulation is an iterative procedure [6] where at first the relative occupations of the subbands are calculated from the Fermi-Dirac distribution [1, 6]

$$N_n=\frac{g_n m_{dn} k_B T}{N_s\pi\hbar^2}\ln\left[1+\exp\left(\frac{E_F-E_n}{k_BT}\right)\right], \tag{21}$$

where g_n is the valley degeneracy and E_F is the Fermi energy. Then the values of N_n are substituted in Eq. (2) and the set of equations (1)—(4) is solved self-consistently. The solution to this system is used to calculate the scattering rates. After the Monte Carlo simulation of the electron ensemble the values of N_n are recalculated as

$$N_n=\sum_l t_{nl}/\sum_{l,n}t_{nl}, \tag{22}$$

where t_{nl} is the total free-flight time of electron l in subband n. Then these recalculated values of N_n are substituted to the equation set (1)—(4), which is solved again with the new N_n. This procedure is iteratively repeated.

The value of the RNSE of the k-th process is calculated according to

$$RNSE_k = n_k / \sum_k n_k, \tag{23}$$

where n_k is the number of events of the k-th scattering process which take place in the ensemble during the time of simulation.

3. Results

The mobility μ as function of the sheet charge carrier density N_s is plotted in Fig. 1. Curve 1 represents the MC result and curve 2 the experimental data from Ref. [10]. A sufficiently good agreement between experimental and simulation data confirms the adequacy of the developed Monte Carlo model of the real electron kinetics.

Further results of calculation of the RNSE for various scattering mechanisms are also presented. In Fig. 2 the values of RNSE are plotted against temperature T at various values of the sheet charge carrier density N_s. This figure shows that the temperature dependences of the RNSE are qualitatively similar for different N_s. The kinetic energy of electrons increases with temperature. This causes an increase of the number of intersubband scattering events so that the relative numbers of e-e and optical phonon scattering events noticeably increase. The more complex behavior of the relative number of ionized impurity scattering events is determined by the "$1 \longrightarrow 0$" intersubband transitions caused by acoustic phonons. Our calculations have shown that the average kinetic energy at $T \approx 230$ K for the case of $N_s = 10^{16}$ m^{-2} and at $T \approx 270$ K for the case of $N_s = 4 \cdot 10^{16}$ m^{-2} is approximately equal to the gap between these two levels. This intersubband transition keeps the electron kinetic energy very low. As the rate of ionized impurity scattering is inversely proportional to E_{kin}, the RNSE of this mechanism increases.

In Fig. 3 the values of the RNSE versus sheet charge carrier density N_s at $T = 77$ K (curve a) and $T = 300$ K (curve b) are presented. This figure in particular shows that the relative number of surface roughness scattering events increases with N_s. In this case the increase of the energy gaps between the subband levels [9] causes a decrease of the relative numbers of phonon and e-e scattering events. The point of intersection of the RNSE curves of the surface roughness and ionized impurity scattering corresponds to the maximum of the function $\mu(N_s)$ at $T = 77$ K (see Fig. 1). This fact is in good agreement with

known theoretical views on the behavior of the function of electron mobility versus electron sheet density [1].

The RNSE as a function of the driving electric field strength F is presented in Fig. 4. The growth of the driving electric field strength increases the RNSE of those processes which decrease kinetic energy, that is in particular optical phonon scattering. In the same figure the electron drift velocity v_{dr} against driving electric field strength F is plotted. It should be noted that the point of intersection of the RNSE for acoustic and optical phonon scattering corresponds to the beginning of the saturation of the drift velocity dependence with respect to the driving electric field strength. This saturation is the consequence of energy loss caused by optical phonon scattering.

4. Conclusions

Results of calculations of the relative numbers of scattering events have been presented. These results show that the relative frequency of each scattering process in a Si-inversion layer can be well characterized by a unique function of temperature, electron sheet density, and driving field strength. The RNSE reflects quantitatively the influence of a particular scattering mechanism on the electron transport.

References

[1] T. Ando, A. Fowler, F. Stern, Rev. Mod. Phys., 54 (1982) 437.

[2] C. Jacoboni, L. Reggiani, Rev. Mod. Phys., 55 (1983) 645.

[3] P.K. Basu, Solid State Comm., 27 (1978) 657.

[4] Chu-Hao, J. Zimmerman, M. Charef, R. Fauquembergue, E. Constant, Solid-St. Electron., 28 (1985) 733.

[5] S. Imanaga, Y. Hayafuji, J. Appl. Phys., 70 (1991) 1522.

[6] M. Shirahata, K. Taniguchi, C. Hamaguchi, Jap. J. Appl. Phys., 26 (1987) 1447.

[7] M.V. Fischetti, S.E. Laux, Phys. Rev., B48 (1993) 2244.

[8] P.J. Price, Ann. Phys., 133 (1981) 217.

[9] S. Yamakawa, H. Ueno, K. Taniguchi, C. Hamaguchi, K. Miyatsu, U. Ravaioli, J. Appl. Phys., 79 (1996) 911.

[10] K. Masaki, Jap. J. Appl. Phys., 28 (1989) 1856.

[11] T.H. Ning, C.T. Sah, Phys. Rev., B6 (1972) 4605.

[12] M. Martisov, A. Shik, Fiz. Tekh. Poluprov., 21 (1987) 1474.

[13] S.M. Goodnick, P. Lugli, Phys. Rev., B37 (1988) 2578.

[14] V. Borzdov, O. Zhevnjak, F. Komarov, Fiz. Tekh. Poluprov., 29 (1995) 95.

[15] Borzdov V.M., Galenchik V.O., Komarov F.F., Phys. Low-Dim. Struct., 5/6 (1998) 73.

[16] V.M. Borzdov, V.O. Galenchik, Phys. Low-Dim. Struct., 3/4 (2000) 19.

[17] V.M. Borzdov, F.F. Komarov, T.A. Petrovich, M.M. Vrubel, O.G. Zhevnyak, Phys. Stat. Sol., 83 (1994) K47.

[18] V. Borzdov, T. Petrovich, Semiconductors, 31 (1997) 89.

[19] F. Gámiz, J.B. Roldán, J.A. López-Villanueva, P. Cartujo-Cassinello, J.E. Carceler, J. Appl. Phys., 86 (1999) 6854.

[20] S.M. Goodnick, R.G. Gann, J.R. Sites, D.K. Ferry, C.W. Wilmsen, D. Fathy, O.L. Krivanek, J. Vac. Sci. Technol., B1 (1983) 803.

[21] D.S Jeon., D.E. Burk, IEEE Trans. Electron Dev., 36 (1989) 1456.